OPTICAL COMPLEX SPECTRUM ANALYZER

Application note :

OPTICAL INTENSITY RESPONSE AND CHIRP PARAMETER OF MACH-ZEHNDER ELECTRO-OPTIC TRAVELING WAVE MODULATORS

Distribution in the UK & Ireland

Lambda

Characterisation, Measurement & Analysis

Lambda Photometrics Limited
Lambda House Batford Mill
Harpenden Herts AL5 5BZ
United Kingdom
E: info@lambdaphoto.co.uk
W: www.lambdaphoto.co.uk
T: +44 (0)1582 764334
F: +44 (0)1582 712084

20/02/2004

INTRODUCTION

The discussion exposed here is based on a synthesis of several elements collected in some papers (see references at the end of the document) dealing with fundamental characteristics of Mach-Zehnder electro-optic traveling wave intensity modulators. We draw an analysis of the optical response of these modulators to a time varying drive voltage, modelized after a description of their technological conception. Then we review the important parameters to study for the use of these modulators in optical transmissions (optical response bandwidth, chirp parameter). We present the properties of these parameters with respect to the previous analysis, and we show that they can be characterized independently, which is of great importance to analyse the performances of such modulators in long haul transmissions.

SCHEMATIC DESCRIPTION OF THE MODULATORS TOPOLOGY

In electro-optic modulators based on Mach-Zehnder interferometer (see fig.1), light entering the input waveguide is split into a pair of separated waveguides integrated in $LiNbO_3$ substrate (the two arms 1 and 2 of the interferometer) and recombined at the other end into a single output waveguide. A differential time varying RF voltage, applied to the arms 1 and 2 with a set of electrodes, changes the relative optical index of the arms by electro-optic effect, thus the relative optical phase of the light traveling through them and therefore the total output power and phase of the recombined optical fields ([3]).

For improved efficiency, the electrodes are close and parallel to the optical waveguides, allowing the RF electrical field to be applied practically all along the waveguides. The longer the waveguides and electrodes, the longer the interaction length between RF and optical fields through the electro-optic medium, and the shorter the RF voltage magnitude required for transition from maximal to minimal output power (ON/OFF). This kind of device is named a traveling wave optical modulator ([1]).

In single drive modulators, the voltage is applied between a single common electrode (the « hot » electrode) and two surrounding electrodes linked to the ground ([1]). In z-cut modulators (see fig.3), the hot electrode is positioned directly above one arm, and one ground electrode above the other arm. The RF field flux concentration is maximal underneath the hot electrode, leading to a strong overlap between RF and optical fields in the corresponding waveguide, whereas their overlap is weaker in the other arm. Thus the induced phase variations are significantly different in magnitude, and opposite in sign, because the RF electrical field has opposite orientation in one arm compared to the other.

In x-cut modulators (see fig.2), the waveguides positions are symmetrical with respect to the electrodes, each one being located between the hot electrode and one ground electrode, leading to similar overlaps between RF and optical fields in both arms. Therefore the induced phase variations are close in magnitude and opposite in sign.

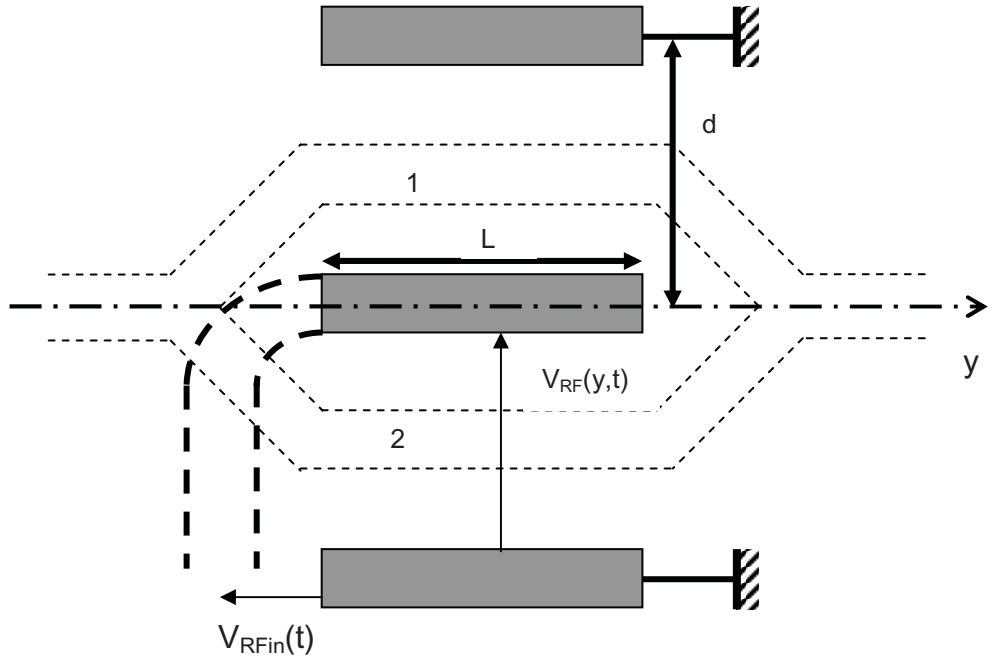

Fig.1 : Mach-Zehnder modulator (x-cut) seen from above

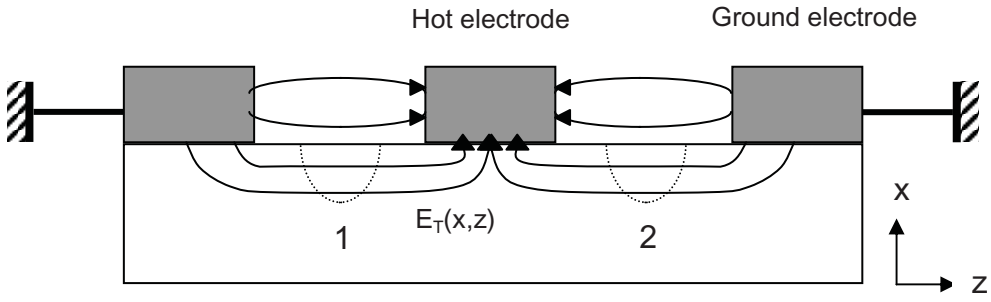

Fig.2 : transversal slice of a x-cut Mach-Zehnder modulator

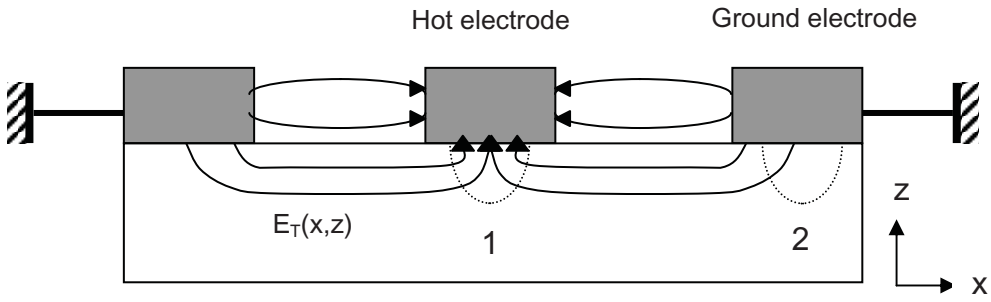

Fig.3 : transversal slice of a z-cut Mach-Zehnder modulator

MODELIZATION OF THE OPTICAL RESPONSE

The optical response of the modulator (i.e. the time variations of the output optical power and phase of the modulated light, for a given input RF voltage) depends on the propagation characteristics of the RF field along the device, as well as the interaction between the RF and optical fields along the waveguides (parallel to the electrodes). The voltage $V_{RF}(y,t)$ between the hot electrode and the ground electrodes (y = longitudinal position along the electrodes axis, t = time) creates a corresponding electrical field $\vec{E}_{RF}(x,y,z,t)$ all over the transversal plane (x,z) centered on position y, and we will consider that $\vec{E}_{RF}(x,y,z,t)$ is proportional to $V_{RF}(y,t)$ and undelayed with respect to it, which implies that the effective transversal dimensions of the device are far smaller than the RF wavelength (thus far smaller than 1 cm for RF frequency = 10 GHz ; usually they are a few hundreds of micrometers [2]). In these conditions, the transversal projection of the RF field (perpendicularly to the propagation axis y) can be decomposed into the product of a pure transversal vectorial function and a pure longitudinal scalar function :

$$\vec{E}_{RF}^{transv.}(x,y,z,t) = \vec{E}_T(x,z)\,f(y,t) \qquad (1)$$

The term $\vec{E}_T(x,z)$ corresponds to the field flux sketched on fig.2 and 3.

RF response : propagation of the RF electrical signal.

The propagation of the RF electrical signal can be represented by the variations of the voltage between the hot electrode and the ground, as a function of y and t :
$V_{RF}(y,t) = V_0 f(y,t)$.

These variations are governed by the following parameters :
* the effective index N_{RF} of the RF wave, which gives its propagation velocity along the device. N_{RF} depends on the dielectric constants of $LiNbO_3$ substrate, as well as the transversal dimensions and positions of the electrodes, and can be significantly modified by the presence of a SiO_2 buffer layer between the electrodes and the substrate ([1], [2]). Its frequency dispersion is negligible ([2]).
* the attenuation experienced by the RF wave due to electrical losses, namely conductor, dielectric and radiative losses ([2]). It is modelized by a frequency dependent attenuation coefficient α_{RF}.
* the reflection coefficient Γ of the RF wave at both sides of the device, due to impedance mismatch. It gives birth to a counterpropragating wave and also modifies the direct copropagating wave because of multiple reflections.

When the voltage V_{RFin} injected at the RF input is purely sinusoïdal with frequency $\Omega/2\pi$, i.e. :
$$V_{RFin}(\Omega,t) = \mathrm{Re}\left\{\tilde{V}_{RFin}(\Omega)e^{j\Omega t}\right\} \qquad (2)$$

then, in the most general case, the voltage propagation function takes the form of two copropagating and counterpropagating sinusoïdal waves :
$$V_{RF}(\Omega,y,t) = \mathrm{Re}\left\{\tilde{V}_{RFin}(\Omega)\left[K_-(\Omega)e^{-\alpha_{RF}y}\exp\left(j(\Omega t-\beta_{RF}y)\right)+K_+(\Omega)e^{\alpha_{RF}y}\exp\left(j(\Omega t+\beta_{RF}y)\right)\right]\right\} \qquad (3)$$

$\beta_{RF} = N_{RF}\,\Omega/c$ (c = speed of light in vacuum) is the propagation constant, $K_-(\Omega)$ and $K_+(\Omega)$ are complex coefficients depending on Γ, $\alpha_{RF}(\Omega)$, $\beta_{RF}(\Omega)$ and the electrodes length L ([2]).

Interaction between RF and optical fields.

The interaction between the RF and optical fields, by mediation of the electro-optic tensor of $LiNbO_3$, has transversal and longitudinal characteristics.

Analysis in the transversal plane :

In the transversal (x,z) plane, the change of the optical index inside the waveguides, induced by the RF electrical field, depends on the location of the waveguides with respect to the field distribution $\vec{E}_T(x,z)$. Since $\vec{E}_T$ is principally oriented along the z-axis of $LiNbO_3$ inside the waveguides, and r_{33} is the greatest electro-optical coefficient of $LiNbO_3$, the local change of the optical index N_o in the arm a (a = 1 or 2) is :

$$\left(\Delta N_o\right)_a = -\frac{N_o^{\,3}}{2} r_{33} \xi_a \frac{V_{RF}}{d} \qquad (4)$$

where d is the distance between the hot and the ground electrodes, and ξ_a is a reduction coefficient representing the transversal overlap between the electrical field $\vec{E}_T(x,z)$ and the light inside the arm. In the case of z-cut modulators (fig.3), with the arm 1 positioned underneath the hot electrode, ξ_1 and ξ_2 have opposite signs with $|\xi_1| > |\xi_2|$ ($|\xi_1|$ is optimized). In the case of x-cut modulators (fig.2), ξ_1 and ξ_2 have opposite signs with $|\xi_1| \approx |\xi_2|$ ([1]).

Analysis along the longitudinal direction of propagation :

Along the propagation axis y, the interaction is impeded by the velocity mismatch between the RF and optical waves, due to the difference between their respective indices ($N_o < N_{RF}$) : the optical wave travels faster than the RF wave, and thus the optical modulation and the RF signal become progressively out of phase during their propagation. This results in bandwidth limitation of the optical response, since this effect becomes more serious at higher frequencies. More generally, one shall express the optical index change seen at y coordinate by a photon entering the arm at instant t_0, all along its propagation at speed c/N_o :

$$\left(\Delta N_o^{photon}\right)_a\left(y,t_0\right) = -\frac{N_o^{\,3} r_{33} \xi_a}{2d} V_{RF}\left(y, t_0 + \frac{y}{c/N_o}\right) \qquad (5)$$

The total phase change experienced by the photon over the interaction length L is :

$$\Delta\Phi_a(t_0) = \frac{2\pi}{\lambda}\int_0^L \left(\Delta N_o^{photon}\right)_a\left(y,t_0\right)dy \qquad (6)$$

At frequency $\Omega/2\pi$ and using eq. (3) for taking the internal reflections of the RF wave into account, the total phase change has the mathematical form as a function of time (eq.(3),(5),(6)) :

$$\Delta\Phi_a(\Omega,t) = \eta_a\,\mathrm{Re}\left\{K(\Omega)\tilde{V}_{RFin}(\Omega)e^{j\Omega t}\right\} \qquad (7)$$

with

$$\eta_a = -\frac{\pi N_o{}^3 r_{33} L}{\lambda d}\xi_a \qquad (8)$$

$$K(\Omega) = \frac{-K_-(\Omega)}{(\alpha_{RF} + j\beta_-)L}\left\{\exp\left[-(\alpha_{RF} + j\beta_-)L\right]-1\right\} + \frac{K_+(\Omega)}{(\alpha_{RF} + j\beta_+)L}\left\{\exp\left[(\alpha_{RF} + j\beta_+)L\right]-1\right\} \qquad (9)$$

$$\beta_\pm = \frac{\Omega}{c}\left(N_{RF} \pm N_o\right) \qquad (10)$$

In the most general case, the input RF signal is not sinusoïdal but composed of several spectral components :

$$V_{RFin}(t) = \mathrm{Re}\left\{\int_\Omega \tilde{V}_{RFin}(\Omega) e^{j\Omega t} d\Omega\right\} \qquad (11)$$

Because of the linearity of the above equations, the resulting phase variation in each arm is :

$$\Delta\Phi_a(t) = \eta_a V_{RFeff}(t) \qquad (12)$$

with

$$V_{RFeff}(t) = \mathrm{Re}\left\{\int_\Omega K(\Omega)\tilde{V}_{RFin}(\Omega) e^{j\Omega t} d\Omega\right\} \qquad (13)$$

$V_{RFeff}(t)$ is the effective voltage interacting with the optical fields in the waveguides, common to both arms of the interferometer, and η_a is a coefficient quantifying the sensitivity of each arm to this voltage.

Recombined output optical field.

The recombined complex optical field at the output of the modulator is :

$$\sqrt{2I(t)}\exp\{j\Phi(t)\} = \sqrt{\frac{I_{\max}}{2}}\left[\sqrt{1-\varepsilon}\exp\{j\Phi_1(t)\} + \sqrt{1+\varepsilon}\exp\{j\Phi_2(t)\}\right] \qquad (14)$$

where ε quantifies the unbalance between the powers transmitted through arms 1 and 2.

Power and phase :

The output power is :

$$I(t) = \frac{I_{\max}}{2}\left[1 + \sqrt{1-\varepsilon^2}\cos\left(\Phi_2 - \Phi_1\right)\right] \qquad (15)$$

It is a function of the phase difference (see eq. (12)) :

$$\Phi_2 - \Phi_1 = \Delta\Phi_0 + (\eta_2 - \eta_1)V_{RFeff}(t)$$

where $\Delta\Phi_0$ is the phase difference with null applied voltage. Because η_1 and η_2 have opposite signs, their difference is non zero : thus one can include $\Delta\Phi_0$ in the DC component of V_{RFeff} and suppose for simplicity that $\Phi_1 = \Phi_2 = 0$ when the drive voltage is zero.

The extinction ratio is : $ER = \dfrac{I_{\max}}{I_{\min}} = \dfrac{1+\sqrt{1-\varepsilon^2}}{1-\sqrt{1-\varepsilon^2}} \approx \dfrac{4}{\varepsilon^2}$ (16)

In standard modulators, the extinction ratio is typically higher than 25 dB, and thus $|\varepsilon| < 0.1$. That is why first order approximation with respect to ε is used in the following calculations.

Far enough from extinction, i.e. as long as this approximation is valid, the output power is :

$$I(t) \approx \frac{I_{\max}}{2}\left[1+\cos\left(\Phi_2-\Phi_1\right)\right] = I_{\max}\cos^2\left(\frac{\Phi_2-\Phi_1}{2}\right) = I_{\max}\cos^2\left(\frac{\eta_2-\eta_1}{2}V_{RFeff}(t)\right) \qquad (17)$$

The output instantaneous optical phase is :

$$\Phi(t) \approx \frac{\Phi_2+\Phi_1}{2} + \frac{\varepsilon}{2}\tan\left\{\frac{\Phi_2-\Phi_1}{2}\right\} = \frac{\eta_2+\eta_1}{2}V_{RFeff}(t) + \frac{\varepsilon}{2}\tan\left\{\frac{\eta_2-\eta_1}{2}V_{RFeff}(t)\right\} \qquad (18)$$

Chirp parameter :

The instantaneous chirp (α) parameter is :

$$\alpha(t) = 2I\frac{d\Phi/dt}{dI/dt} \approx \frac{(d\Phi_1/dt)+(d\Phi_2/dt)}{(d\Phi_1/dt)-(d\Phi_2/dt)}\cot\left(\frac{\Phi_2-\Phi_1}{2}\right) - \frac{\varepsilon}{\sin(\Phi_2-\Phi_1)}$$

$$\alpha(t) \approx \frac{\eta_1+\eta_2}{\eta_1-\eta_2}\cot\left(\frac{\eta_2-\eta_1}{2}V_{RFeff}(t)\right) - \frac{\varepsilon}{\sin\left((\eta_2-\eta_1)V_{RFeff}(t)\right)} \qquad (19)$$

At half maximal output power ($I = I_{max}/2$), i.e. when $\Phi_2-\Phi_1 = \pm\pi/2$:

$$\alpha_{50\%} \approx \pm\left(\frac{\eta_1+\eta_2}{\eta_1-\eta_2} - \varepsilon\right) = \pm\left(\frac{\xi_1+\xi_2}{\xi_1-\xi_2} - \varepsilon\right) \qquad (20)$$

(see eq. (8))

Note that this value is only a function of static parameters of the modulator (no one depends on the RF frequency $\Omega/2\pi$ introduced above) and thus it is independent of the input RF signal.

$\alpha_{50\%}$ can also be used to predict the time variations of the optical phase $\Phi(t)$ when knowing those of the power $I(t)$. By using relation (20) and taking the value $\alpha_{50\%}$ measured at $\Phi_2-\Phi_1 = +\pi/2$, eq. (17) and (18) can be rewritten into the following parametric system :

$$I = I_{\max}\cos^2\varphi \qquad (21)$$

$$\Phi = -\left(\alpha_{50\%}+\varepsilon\right)\varphi + \frac{\varepsilon}{2}\tan\varphi \qquad (22)$$

with $\varphi(t) = \frac{\Phi_2-\Phi_1}{2} = \frac{\eta_2-\eta_1}{2}V_{RFeff}(t)$

which provides for a direct relation between Φ and I.

ε, whose absolute value can be roughly estimated by the extinction ratio (eq. (16)), is usually weak with respect to $\alpha_{50\%}$ and thus its influence can be neglected. Taking ε into account for a very accurate analysis is difficult, because its sign and its accurate absolute value are not easy to determine (this problem is not treated here).

Note that eq.(21),(22) are not valid when I is close to its minimal value (extinction) : here (21) should be replaced by (15), and the approximations leading to (22) are no longer valid since Φ

would become infinite when $\varphi = \pm\pi/2$. But the definition of the phase is of poor importance when the optical power approaches zero.

APPLICATION TO MODULATORS CHARACTERIZATION FOR OPTICAL TRANSMISSIONS

Two important characteristics are relevant for using a modulator as an optical transmitter, especially for long haul fiber communications.

Bandwidth of the optical response.

Its optical response will determine how the modulated signal generated at the optical output of the device will be distorded, with respect to the input drive voltage corresponding to a binary sequence synthetized by an electronic pulse pattern generator. The bandwidth requirements are especially high for today's standard bit rates, 10 or even 40 Gbits per second. That's why many efforts have been made for optimizing the bandwidth, in particular by reducing the velocity mismatch between the optical and the drive signals ([1], [2]).

The full bandwidth characterization can be done by applying a small sinusoïdal RF drive voltage at different frequencies $\Omega/2\pi$, around a DC bias voltage fixed at half maximal power transmission, so that the transmission function (I as a function of V_{RFeff}) is practically linear (see eq. (17)) and measuring the amplitude and phase of the modulated output power with respect to those of the drive voltage. This experiment can provide for the measurement of $(\eta_2 - \eta_1)K(\Omega)$, where $K(\Omega)$ are the spectral Fourier coefficients of the RF response ($V_{RFeff}(t)$ as a function of $V_{RFin}(t)$: see eq. (13)). Then the optical power response can be calculated with eq. (17).

Optical chirp.

The chirp is another important parameter because it will cause the distortion of the modulated optical signal along its propagation through a long distance of fiber, because of chromatic dispersion (and non linear effects also, even if they are less important). Many studies have been carried to study the impact of chirp in term of dispersion penalty, and the chirp parameter (α) appears to be a relevant figure of merit. It represents the relative amount of phase variations with respect to power variation (like shown in eq. (19)) but it is constant only in small-signal modulation regime. For large signal modulation like it is used in fiber communications, the definition of the real value that should be used is quite fuzzy, and several effective α parameters have been studied and compared ([4]), showing that no one of these values can accurately characterize the absolute performances of the modulator for fiber transmissions, because a single parameter is not enough for this.

However, the value given here ($\alpha_{50\%}$ in eq. (20)), which characterizes small-signal modulation regime around half maximal transmission, can be used for *comparing* performances of several modulators, like it is shown in [3] and [5]. The very important property of this kind of modulators is that $\alpha_{50\%}$ does not depend on the RF frequency, and thus, for instance, if two modulators have two different values $\alpha_{50\%}(1)$ and $\alpha_{50\%}(2)$, their comparison can permit to predict the resulting variations of the BER or power penalty after transmission through

dispersive fiber line with a PRBS modulating signal, even if $\alpha_{50\%}(1)$ and $\alpha_{50\%}(2)$ have not been measured with a PRBS signal.

For a complete analysis of the output signal and its transmission through the dispersive fiber, one can measure the optical intensity with a scope (or calculate it by characterization of the optical response bandwidth), and then calculate the corresponding optical chirp by means of the parameter $\alpha_{50\%}$ (see eq. (21),(22)).

EXAMPLES OF CHIRP PARAMETER MEASUREMENTS

Graphs 1 and 2 show time variations of the modulated optical power at the output of a single-drive lithium niobate 10 Gb/s Mach-Zehnder modulator, and the corresponding chirp parameter (alpha). These profiles have been measured with AP1040A chirp analyzer (Apex Technologies), applying 4 bits periodical patterns (resp. 1000 and 1110) at about 10 Gb/s to the input RF port of the modulator. Line markers V1 and V2 are positioned at approximately half maximal power on the leading and the falling edges of the pulse, and line marker H1 shows the corresponding alpha value ($\alpha_{50\%}$), which is nearly the same (about -1) at both edges and for both patterns.

Note :

This discussion is stricly valid for single-drive modulators but may be extended to dual-drive modulators if the RF spectral response is similar for both drives.

References :

[1] E.L. Wooten, K.M. Kissa, A. Yi-Yan, E.J. Murphy, D.A. Lafaw, P.F. Hallemeier, D. Maack, D.V. Attanasio, D.J. Fritz, G.J. MacBrien, D.E. Bossi, « A Review of Lithium Niobate Modulators for Fiber-Optic Communications Systems », *IEEE Journal of Selected Topics in Quantum Electronics*, Vol. 6, pp. 69-82 (2000).

[2] G.K. Gopalakrishnan, W.K. Burns, R.W. MacElhanon, C.H. Bulmer, A.S. Greenblatt, « Performance and Modeling of Broadband $LiNbO_3$ Traveling Wave Optical Intensity Modulators », *Journal of Lightwave Technology*, Vol. 12, pp. 1807-1819 (1994).

[3] F. Heismann, S.K. Korotky, J.J. Veselka, « Lithium Niobate Integrated Optics : Selected Contempary Devices and System Applications », in *Optical Fiber Communications IIIB*, Ed. I.P. Kaminow and T.L. Koch (Academic Press), Chap. 9, pp. 377-462 (1997).

[4] J.C. Cartledge, « Comparison of Effective α-Parameters for Semiconductor Mach-Zehnder Optical Modulators », *Journal of Lightwave Technology*, Vol. 16, pp. 372-379 (1998).

[5] « The Relationship Between Chirp and Voltage for the AT&T Mach-Zehnder Lithium Niobate Modulators », AT&T Microelectronics Technical Note (October 1995).

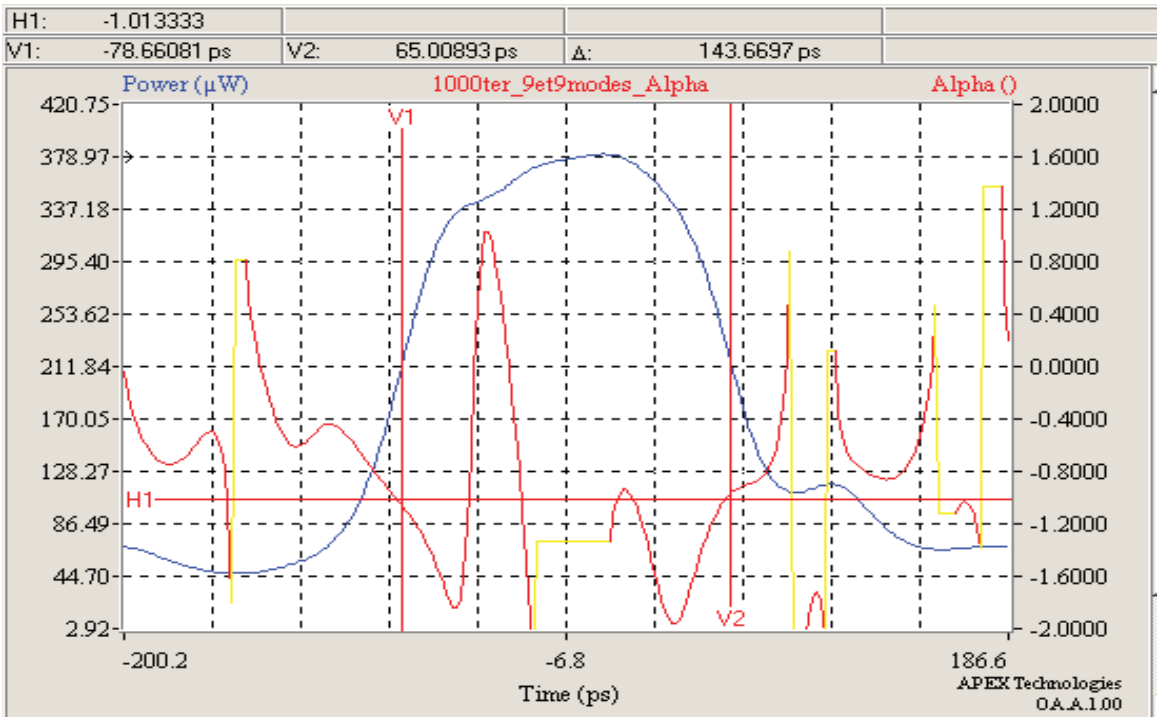

<u>Graph 1 :</u> optical power and chirp parameter (alpha) at the output of a Mach-Zehnder lithium niobate single drive modulator ; drive voltage = 4 bits periodical pattern (1000) at about 10 Gbits per second.

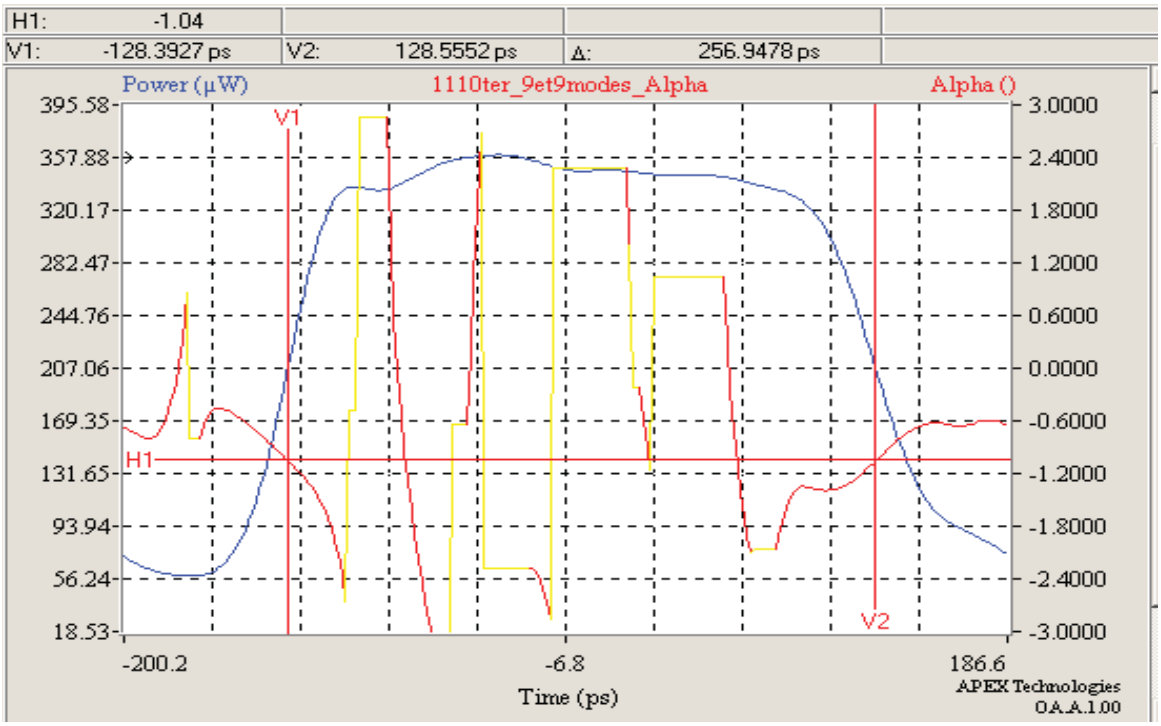

<u>Graph 2 :</u> optical power and chirp parameter (alpha) at the output of a Mach-Zehnder lithium niobate single drive modulator ; drive voltage = 4 bits periodical pattern (1110) at about 10 Gbits per second.

APEX Technologies Products portfolio

AP2040A series Ultra-high resolution Optical Spectrum Analyzer

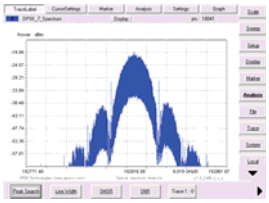

AP2440A series Complex Spectrum Analyzer

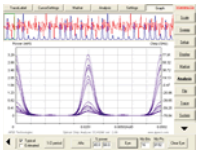

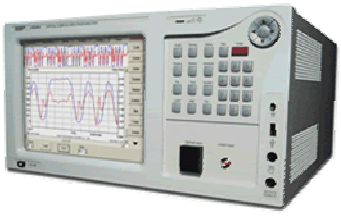

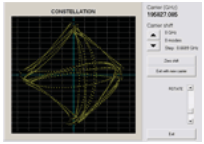

AP2540A series Multi-channel Optical Spectrum Analyzer

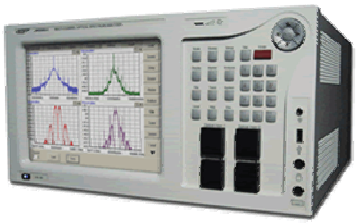

AP3010series and AP3110series high power hand-held power meters

Contacts :

Apex Technologies
9bis, rue Angiboust
91460 MARCOUSSIS
FRANCE
Tel : +33 1 69 63 26 30
Fax : +33 1 69 63 26 37
Email : info@apex-t.com
Web site : www.apex-t.com

Apex Technologies USA
501-I South Reino Road #332
Newbury Park - CA91320
USA
Tel : +1 805 277 0628
Fax : +1 805 277 0632
Email : apex.usa@apex-t.com